



Interferometric study of the class I methanol masers at 104.3 GHz

M. A. Voronkov¹ , S. L. Breen², S. P. Ellingsen³ , A. M. Sobolev⁴
and D. A. Ladeyschikov⁴

¹CSIRO Space & Astronomy, PO Box 76, Epping, NSW 1710, Australia.
email: Maxim.Voronkov@csiro.au

²SKAO, Jodrell Bank, Lower Withington, Macclesfield, Cheshire SK11 9FT, UK

³School of Natural Sciences, University of Tasmania, Private Bag 37, Hobart, Tasmania 7001, Australia

⁴Ural Federal University, 19 Mira street, 620002 Ekaterinburg, Russia

Abstract. The Australia Telescope Compact Array (ATCA) has been used for an interferometric follow up observation at 104.3 GHz of the targets where either this or the 9.9-GHz maser was previously detected. We confirm the significant difference (by more than 1.5 orders of magnitude) from source to source of the flux density ratio for these two maser transitions. Based on the morphology and location of continuum sources, the most likely explanation of this discrepancy is the difference in the flux density of the seed radiation at the two frequencies. We also report absolute positions (with arcsec accuracy) for all detected 104.3 GHz masers.

Keywords. masers, stars: formation, HII regions

1. Introduction

Methanol masers tend to form series of transitions with different members of the series sharing similar observational properties such as whether they can be detected in a particular region of high-mass star formation (e.g., [Cragg *et al.* 1992](#), and references therein). This work is about the $J_{-1}-(J-1)_{-2}$ E transition series which is responsible for the rare class I (or collisionally pumped) methanol masers at 9.9 ($J=9$) and 104.3 GHz ($J=11$). Despite the scarcity of the 104.3-GHz observations, there were reasons to suspect that significant variations from one source to another may be present in the flux density ratio of the two transitions. In particular, no 104.3-GHz maser has been detected towards 9.9-GHz maser in G331.13–0.24. On the other hand, the 9.9-GHz maser in G305.21+0.21 was only a marginal detection despite the presence of the 104.3-GHz maser in this source. In addition, the majority of 104-GHz data were obtained using assorted single dish facilities and no accurate positions have been measured. Therefore, we used the ATCA at 104.3 GHz to image all six targets known to have a maser in this series at the time of our observations (note, four additional 104.3-GHz masers were since reported, see [Yang *et al.* 2023](#), and also a paper in this volume).

2. Results

Fig. 1 shows the environment, including the distribution of the widespread class I methanol masers at 36 and 44 GHz from [Voronkov *et al.* \(2014\)](#), for two selected sources, G305.21+0.21 and G331.13–0.24. As expected, the rare $J_{-1}-(J-1)_{-2}$ E masers appear in a single location at this scale. The noteworthy feature of these maps is that the

Table 1. Sources observed at 104.3 GHz in this project and the 9.9 GHz flux density from the literature for comparison. The measurement uncertainties are given in the brackets and expressed in the units of the least significant figure. For the two sources marked with (*), this result is the first measurement of the absolute position with an arcsecond accuracy for any maser in this series.

Source	Absolute position (J2000)		Peak	Peak flux density	
	Right Ascension	Declination	V_{LSR}	104 GHz	9.9 GHz
	(h:m:s)	(deg:arcmin:arcsec)	km s ^{−1}	Jy	Jy
G305.21+0.21*	13:11:10.83 (7)	−62:34:38.5 (5)	−42.3 (1)	21.3 (6)	≤ 0.2 ^[1]
G331.13−0.24	Non-detection at 104.3 GHz, single channel rms noise is 0.84 Jy				~3 ^[1,2]
G343.12−0.06	16:58:16.46 (5)	−42:52:25.5 (5)	−31.7 (1)	14.9 (7)	9.5 (3) ^[3]
G357.97−0.16*	17:41:20.06 (4)	−30:45:18.3 (5)	−5.0 (1)	15.8 (9)	69 (2) ^[4]
G012.80−0.19	18:14:10.90 (4)	−17:55:58.8 (5)	+32.9 (1)	10 (2)	4.3 (1) ^[1]
G019.61−0.23	18:27:37.49 (4)	−11:56:38.6 (5)	+41.3 (1)	9 (1)	3.3 (1) ^[1]

Source of the 9.9 GHz data: [1] Voronkov *et al.* (2010), [2] Voronkov *et al.* (this volume), [3] Voronkov *et al.* (2006), [4] Voronkov *et al.* (2011)

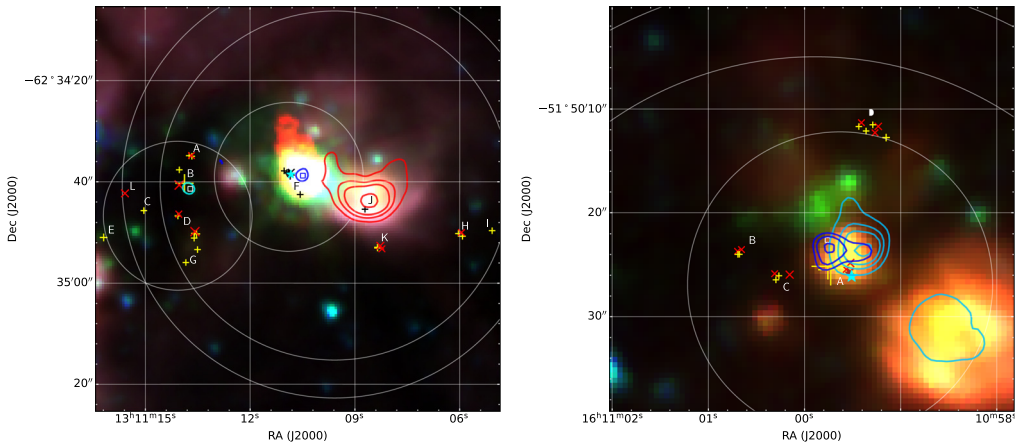


Figure 1. Two selected sources from the project: G305.21+0.21 (left) and G331.13−0.24 (right). The images are derived from that of Voronkov *et al.* (2014) and have the measured position of a J_{−1}–(J−1)_{−2} E maser (either 104 or 9.9 GHz, as appropriate) shown by the star symbol along with the 3mm and 3cm continuum emission (small and large contours, respectively). As in the original images, the location of the 36 (crosses) and 44 GHz (pluses) masers are shown on top of the Spitzer 3-colour background (8.0, 4.5 and 3.6 μm images are shown as red, green and blue, respectively). The large circles represent the primary beam FWHM and pointing directions for 36, 44 and 104 GHz observations (the 9.9 GHz beam is too wide to show, with the whole field being well within the FWHM).

104.3-GHz maser in G305.21+0.21 is located near the 3-mm continuum source and far away from the 3-cm one. The opposite is observed in G331.13−0.24, where the 9.9-GHz maser is seen projected onto an HII region prominent at 3-cm, but offset from the 3-mm continuum source. Therefore, we conclude that it is the difference in the seed radiation at notably different frequencies of these two maser transitions (the emission at these two frequencies is produced by an HII region or a dust emission source which are not necessarily co-located) which is responsible for the observed relative flux densities in these two sources and may be a contributing factor for the other sources (Table 1). It is worth noting that no continuum emission at either of these frequencies has been detected at a position of a very strong 9.9-GHz maser in G357.97−0.16, quite possibly due to an insufficient sensitivity.

Supplementary material

To view supplementary material for this article, please visit <http://dx.doi.org/10.1017/S1743921323001953>

References

- Cragg, D. M., Johns, K. P., Godfrey, P. D., Brown, R. D. 1992, *MNRAS*, 259, 203
Voronkov, M. A., Brooks, K. J., Sobolev, A. M. *et al.* 2006, *MNRAS*, 373, 411
Voronkov, M. A., Caswell, J. L., Ellingsen, S. P., Sobolev, A. M., 2010, *MNRAS*, 405, 2471
Voronkov, M. A., Walsh, A. J., Caswell, J. L., *et al.* 2011, *MNRAS*, 413, 2339
Voronkov, M. A., Caswell, J. L., Ellingsen, S. P., *et al.* 2014, *MNRAS*, 439, 2584
Yang, W., Gong, Y., Menten, K. M. *et al.* 2023, *A&A*, in press (arXiv:2305.04264)